Competition of local exponents and the fractal structure of chaotic attractors

Gerold Baier

Institute for Chemical Plant Physiology, University of Tübingen, Tübingen, Germany

Achim Kittel

Physical Institute, University of Tübingen, Tübingen, Germany

Michael Klein*

Institute for Physical and Theoretical Chemistry, University of Tübingen, Tübingen, Germany

The coupling of a one-dimensional chaotic forcing to a stable fixed point in the plane generates different fractal attractors embedded in three dimensions. There are *three* types of fractals for the fixed point with real eigenvalues and *four* types of fractals for the fixed point with complex eigenvalues in the volume-contracting case. A competition of local exponents provides a generic criterion for the classification of the fractal structures in dynamical systems.

PACS number(s): 05.45.+b, 02.40.−k, 02.60.−x

I. INTRODUCTION

Three-variable discrete diffeomorphisms may possess two different types of chaotic dynamics. These are distinguishable by means of their spectrum of Lyapunov characteristic exponents (LCE's), i.e. $(+,-,-)$ for ordinary chaos and $(+,+,-)$ for hyperchaos [1].

In the case of ordinary chaotic attractors, three types of fractal structures have been described [3], namely, the Cantor set of an infinitely often folded line (*Hénon* attractor [2]), the Cantor set of a smooth sheet folded in one direction (chaotic attractor fulfilling the *Kaplan-Yorke* conjecture [7]), and a structure with nowhere differentiable properties in two directions (*bifractal* attractor [4]). The transitions between these types of chaotic attractors occur at $\Lambda_1+\Lambda_2=0$ and $\Lambda_1+\Lambda_3=0$, respectively, where $\Lambda_1 \geq \Lambda_2 \geq \Lambda_3$ are ordered LCE's with $\sum_i \Lambda_i < 0$, $i=1,2,3$ (see Fig. 1). Thus the fractal structure of chaotic attractors in three-dimensional maps can be predicted from the relation of the *global* means of divergence (positive exponent) and the means of convergence (negative exponents) classified by their respective sums [4].

In the case of basin boundaries modeled with a chaotic dynamics coupled to a bistable variable, it was conjectured that the different fractal structures of the boundary are determined by the competition of the *local* divergence of the chaotic forcing *tangential* to the boundary and the local divergence *orthogonal* to the boundary [5,6]. Similarly, we have argued that fractal features of ordinary chaotic attractors can be explained by the competition of the *local* divergence along the unstable manifold and the local convergence along the stable manifolds [3].

Here we consider a discrete dynamical system with LCE spectrum $(+,-,-)$. We investigate the general case of coupling a chaotic variable to a two-dimensional subsystem with an attracting fixed point. We demonstrate that the *global* fractal structure of chaotic attrac-

tors of the map is obtainable from the knowledge of *local* exponents on the attractive orbit.

II. THE MAP

A simple three-variable map which realizes coupling of a one-dimensional chaotic forcing to a two-dimensional fixed point system is Eq. (1):

$$x_{i+1}=(Cx_i)\mathrm{mod}1 \;,$$

$$y_{i+1}=\epsilon x_i + Ay_i - Bz_i \;,$$

$$z_{i+1}=y_i \;,$$

(1)

with variables $x,y,z \in \mathbb{R}$ and parameters $A,B,C,\epsilon \in \mathbb{R}$, $i \in \mathbb{N}$. The modular variable x is the chaotic forcing with local divergence $\lambda_1=C$, $C>1$ in the interval $[0,1]$ and LCE $\Lambda_1=\ln C$. We took the piecewise linear system only for the direct computability of the Lyapunov exponents from the eigenvalues without averaging the local exponents. We state at this point that similar results are
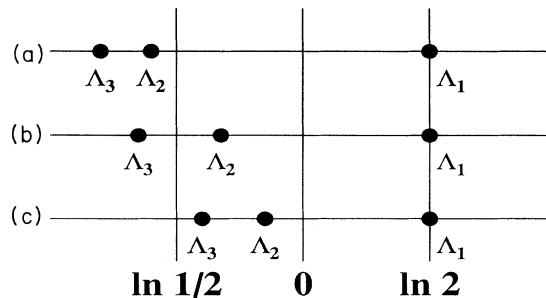

FIG. 1. Three different LCE spectra $(\Lambda_1 \geq \Lambda_2 \geq \Lambda_3)$ for three-variable maps with chaotic attractors, Λ_1 assumed to be ln2: (a) Ordinary chaos $(\Lambda_1 > 0$ only), (b) Kaplan-Yorke chaos $[(\Lambda_1+\Lambda_2)>0$ only], (c) "bifractal" chaotic attractor $[(\Lambda_1+\Lambda_2)>0$ and $(\Lambda_1+\Lambda_3)>0]$.
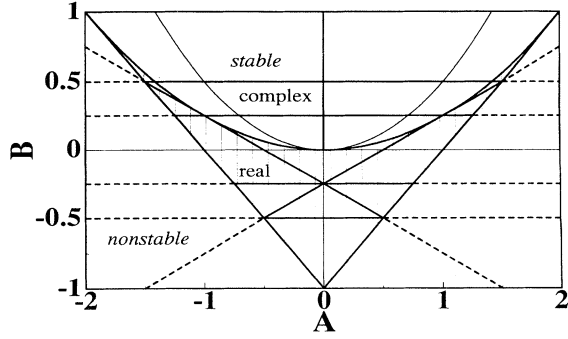
FIG. 2. Parameter plane (A,B) for the subsystem (y,z) of Eq. (1). Lower parabola $B = A^2/4$ transition between complex eigenvalues (focal fixed point) and real eigenvalues (nodal fixed point); line $B = 1$, upper limit of stability in the case of complex eigenvalues; lines bounding triangular area $[|A|=(B+1)]$, lower limit of stability in the case of purely real eigenvalues; horizontal lines at $(|B|=0.5)$, transition to noninvertibility $|\lambda_2|\,|\lambda_3|=|\lambda_1|^{-1}$ and $\prod_i|\lambda_i|=1$; horizontal lines at $(|B|=0.25)$, Kaplan-Yorke transition for the case of equal absolute values of eigenvalues $(|\lambda_2^c|=|\lambda_3^c|)$; diagonally crossing lines, Kaplan-Yorke transition for the case of independent eigenvalues $(\lambda_2^c,\lambda_3^c)$; upper parabola $B = A^2/2$, line of equality of real and imaginary parts of eigenvalues $\text{Re}(\lambda_2)=\text{Im}(\lambda_2)$ and $\text{Re}(\lambda_3)=-\text{Im}(\lambda_3)$.

obtainable with chaotic forcing of the type of the logistic map or the Hénon map.

For $\epsilon=0$, the linear two-variable subsystem (y,z) has a fixed point at the origin with eigenvalues:

$$\lambda_{2,3}=\tfrac{1}{2}(A\pm\sqrt{A^2-4B})\ . \tag{2}$$

Figure 2 shows part of the (A,B) parameter plane of the (y,z) subsystem [Eq. (1)]. The lower parabola $B = A^2/4$ marks the transition between complex eigenvalues $(\lambda_2^c,\lambda_3^c)$ and real eigenvalues $(\lambda_2^r,\lambda_3^r)$. The fixed point is a focus above this parabola and a node $[\text{Im}(\lambda_2)=\text{Im}(\lambda_3)=0]$ below. The complex eigenvalues define an upper limit for the window of stability $(|\lambda_2^c|,|\lambda_3^c|<1)$ in parameter space with $B\le 1$. The purely real eigenvalues restrict the window of stability $(|\lambda_2^r|,|\lambda_3^r|<1)$ to a triangular area in parameter space with $|A|<(B+1)$.

III. COMPETITION OF DIVERGENCE AND CONVERGENCE

Coupling of the chaos-generating variable x to the stable fixed point $(\epsilon>0)$ leads to attractors with LCE's $\Lambda_i=\ln|\lambda_i|$ $(i=1,2,3)$, and the LCE spectrum $(+,-,-)$ where local conditions are simply controllable by means of parameters.

We first give the case when both eigenvalues of the fixed point $(\lambda_2^r$ and $\lambda_3^r)$ are real.

(a) For $\lambda_1\lambda_2^r<1$ the attractor consists of a Cantor set of lines with fractal dimension $1<D_f<2$.

(b) A transition occurs at $\lambda_1\lambda_2^r=1$, which is the Kaplan-Yorke conjecture postulating an increase in fractal dimension [7]. For $\lambda_1\lambda_2^r>1$ and $\lambda_1\lambda_3^r<1$, the attractor is a Cantor set of a folded smooth sheet with dimension

$2<D_f<3$.

(c) A second transition occurs at $\lambda_1\lambda_3^r=1$. For $\lambda_1\lambda_3^r>1$ (with $\prod_i\lambda_i<1$) the structure of the attractor was shown to have a "bifractal" structure [4]. Its fractal dimension remains in between $2<D_f<3$ but the chaotic attractor is fractalized in the orthogonal directions along the stable manifolds. The two contracting local exponents $|\lambda_2^r|$ and $|\lambda_3^r|$ are both smaller than the local divergence $|\lambda_1|$ parallel to the unstable manifold.

These cases support the classification given in Fig. 1.

Next we study the case when the eigenvalues of the fixed point $(\lambda_2^c,\lambda_3^c)$ are complex conjugated $[\text{Im}(\lambda_2^c)=-\text{Im}(\lambda_3^c)]$. Figure 3 shows the first quadrant of the complex plane of eigenvalues $(\lambda_2^c,\lambda_3^c)$. The stable domain of the map, Eq. (1), is bounded by the unit circle $(|\lambda_2^c|,|\lambda_3^c|=1)$ (Fig. 3; compare Fig. 2).

Inside the stable domain there are *three* regions of attractive behavior depending on the products of the absolute values of the eigenvalues $|\lambda_i|$. The corresponding rate of divergence for the chaos is defined as $|\Lambda_1|$, and the rates of contraction in both stable directions of the subsystem (y,z) are $|\Lambda_2|,|\Lambda_3|$, with $\Lambda_i=\ln|\lambda_i|$.

If $|\lambda_2|=|\lambda_3|<|\lambda_1|^{-1}$ then both rates of contraction $|\Lambda_2|$ and $|\Lambda_3|$ exceed the rate of divergence $|\Lambda_1|$. For $\epsilon\neq0$ the resulting attractors for the system of equations (1), are Cantor sets of folded lines, the cross sections of which form self-similar dust [Figs. 4(a), 4(d), and 4(g)]. For nonzero eigenvalues λ_2 and λ_3, the dimension of the fractal attractor is $1<D_f<2$.

At $|\lambda_2|=|\lambda_3|=|\lambda_1|^{-1}$ the rates of convergence $|\Lambda_2|,|\Lambda_3|$ equal the rate of divergence $|\Lambda_1|$. The competition of divergence and the two directions of attraction is balanced (circle with radius $\frac{1}{2}$ in Fig. 3). At this point of the Kaplan-Yorke transition, the attractor dimension is $D_f=2$. Note, however, that the Kaplan-Yorke criterion is fulfilled for both $|\Lambda_2|$ and $|\Lambda_3|$; therefore the first and the second transitions of structure mentioned above
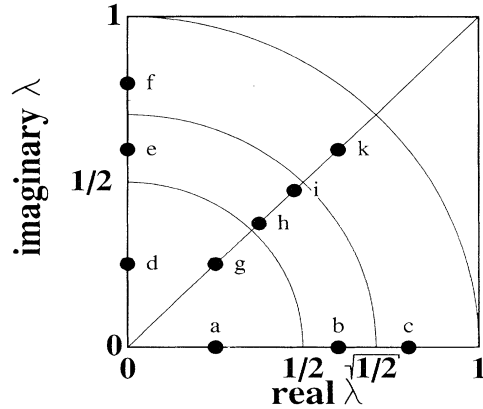

FIG. 3. First quadrant of the complex plane for eigenvalues λ_2^c,λ_3^c, assuming $\lambda_1=2$. Bullets indicate values for cross sections shown in Fig. 4. Outer circle, $|\lambda_2|,|\lambda_3|=1$, area-preserving subsystem (y,z); inner circle, $|\lambda_2|=|\lambda_3|=|\lambda_1|^{-1}$, the Kaplan-Yorke transition; middle circle, $|\lambda_2|=|\lambda_3|=|\lambda_1|^{-1}$ and $\prod_i|\lambda_i|=1$ as transition to noninvertibility.

occur together. In the domain $|\lambda_2|=|\lambda_3|>|\lambda_1|^{-1}$ and $|\lambda_2|\,|\lambda_3|<|\lambda_1|^{-1}$ the rates of convergence $|\Lambda_2|$ and $|\Lambda_3|$ are smaller than the rate of divergence $|\Lambda_1|$. This causes attractor structures to form fractalized distorted sheets. The attractors have fractal dimension $2<D_f<3$. In addition, they are fractalized in two directions [Figs. 4(b), 4(e), 4(h), and 4(i)].

The product $|\lambda_2|\,|\lambda_3|=|\lambda_1|^{-1}$ implies $\prod_i|\lambda_i|=1$ (circle with radius $\sqrt{1/2}$ in Fig. 3). The corresponding attractors have dimension $D_f=3$. For $|\lambda_2|\,|\lambda_3|>|\lambda_1|^{-1}$

the system of equations (1) still possesses attractors but can no longer be embedded in three invertible map dimensions [see Figs. 4(c), 4(g), and 4(k)]. At least four variables are now required to generate the corresponding diffeomorphism.

The cross sections of attractors of Eq. (1) plotted in Fig. 4 are examples picked along three paths (compare Fig. 3) in the complex plane of the complex conjugated eigenvalues λ_2 and λ_3 with $\Lambda_2=\Lambda_3=\ln|\lambda_2|$. For all examples the LCE of the chaotic forcing is fixed to
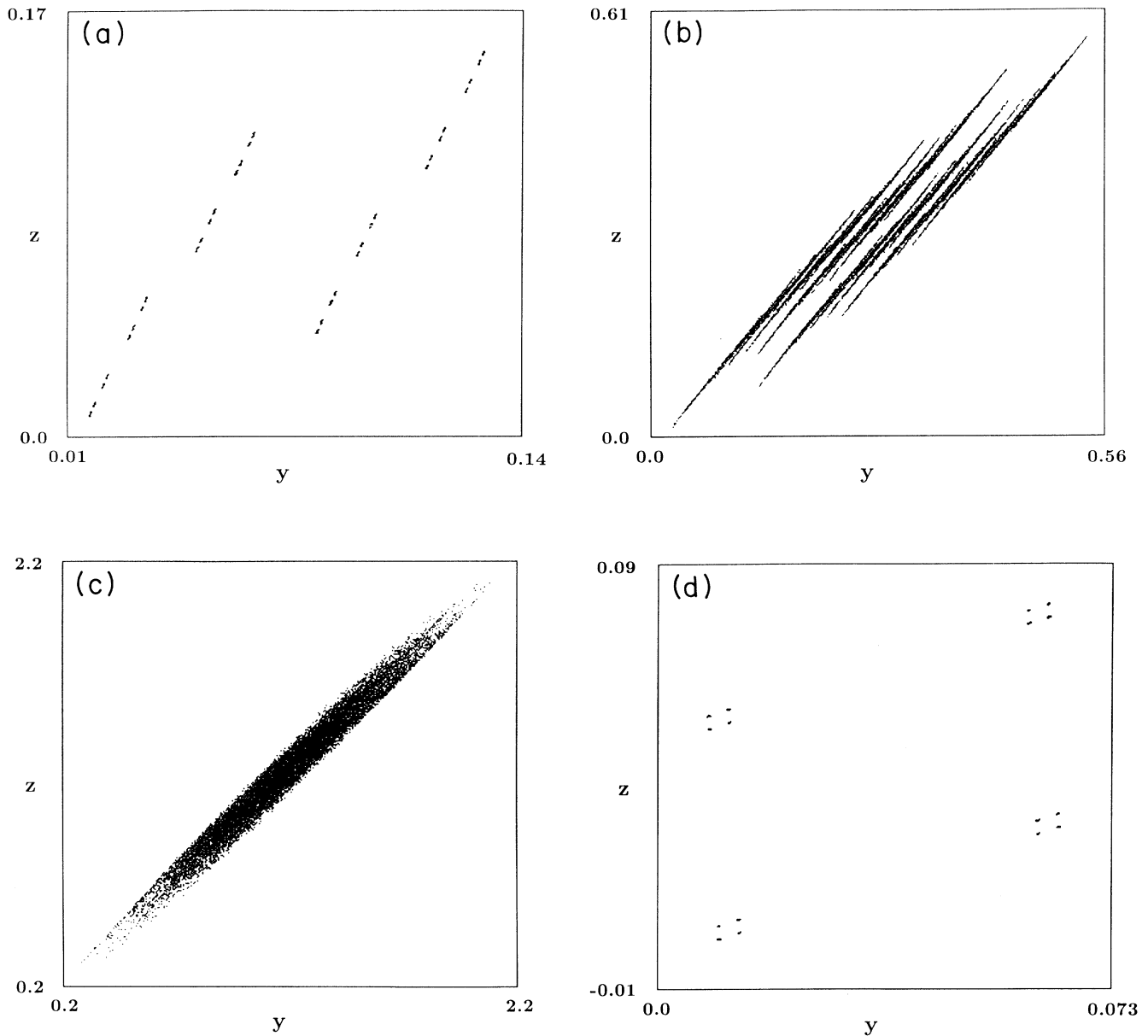

FIG. 4. Cross sections of attractors taken at $x=0.25\pm0.003$ of Eq. (1) with $C=2.0$ and $\epsilon=0.1$. See text and Fig. 3 for corresponding eigenvalues. (a) $A=0.5$, $B=0.0625$ dustlike; (b) $A=1.2$, $B=0.36$ striated; (c) $A=1.6$, $B=0.64$ striated fat; (d) $A=0.0$, $B=0.0625$ dustlike; (e) $A=0.0$, $B=0.36$ checkered; (f) $A=0.0$, $B=0.64$ checkered fat; (g) $A=0.5$, $B=0.125$ dustlike; (h) $A=0.75$, $B=0.28125$ spiral-like disconnected; (i) $A=0.95$, $B=0.45125$ spiral-like connected; (j) $A=1.2$, $B=0.72$ fat spirals.
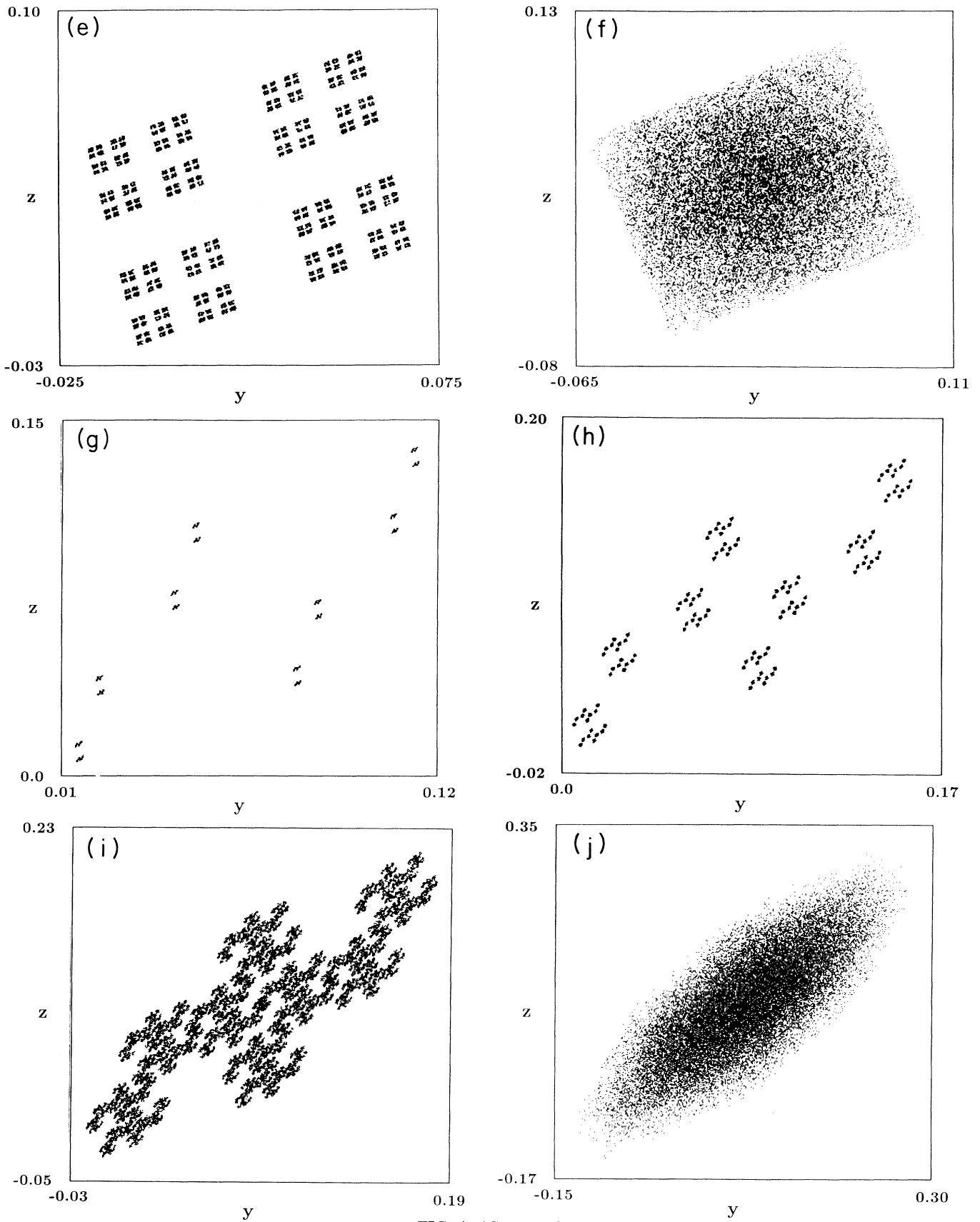
FIG. 4. (Continued).

$\Lambda_1 = \ln\lambda_1 = \ln 2$.

Along the real axis $[B = A^2/4, \Lambda_2 = \ln(A/2)]$ (horizontal axis with $0 < \lambda_2^r < 1$ in Fig. 3 and path with $0 < A < 1, B = 0$ in Fig. 2) there are transitions from dustlike [Fig. 4(a), $A = 0.5, D_f = 1.5$], to striated [Fig. 4(b), $A = 1.2, D_f = 2.36 \cdots$], to striated fat fractal structures [Fig. 4(c), $A = 1.6, D_f = 3.0$].

Along the imaginary axis ($A = 0.0, \Lambda_2 = \ln\sqrt{B}$) [vertical axis with $0 < \text{Im}(\lambda_2^c) < 1$ in Fig. 3 and path with $0 < B < 1, A = 0$ in Fig. 2] the transitions occur from dustlike [Fig. 4(d), $B = 0.0625, D_f = 1.5$], to checkered [Fig. 4(e), $B = 0.36, D_f = 2.36 \cdots$] and finally to checkered fat fractal cross sections [Fig. 4(f), $B = 0.64, D_f = 3.0$].

Moving along the diagonal axes of the complex plane $[B = A^2/2, \Lambda_2 = \ln(A/\sqrt{2})]$ [path with $0 < \text{Re}(\lambda_2^c) = \text{Im}(\lambda_2^c) < 1/\sqrt{2}$ in Fig. 3 and upper parabola in Fig. 2] one finds a transition from dustlike [Fig. 4(g) $A = 0.5, D_f = 1.6$], to spiral-like structures [Fig. 4(h), $A = 0.75, D_f = 2.09\ldots$; Fig. 4(i), $A = 0.95, D_f = 2.74\ldots$], and then to fat spirals [Fig. 4(k), $A = 1.2, D_f = 3.0$].

In the region where $|\lambda_2| = |\lambda_3| > |\lambda_1|^{-1}$ and $|\lambda_2| \, |\lambda_3| < |\lambda_1|^{-1}$ the numerical cross sections either form a single entity [Fig. 4(i) on the diagonal] or are composed of isolated islands [Fig. 4(e) on the imaginary axes; Fig. 4(h) on the diagonal].

IV. DISCUSSION

Competition of rates of local divergence and local convergence explains the fractal properties of chaotic attractors. The map equation (1) composed of one chaotic forcing variable and a two-dimensional subsystem with an attracting fixed point generates the fractal structures possible in three-dimensional maps with the LCE spectrum $(+, -, -)$. When both rates of convergence (Λ_2, Λ_3) exceed the rate of divergence (Λ_1) the dynamics takes place on smooth attractors with Cantor-set-like cross sections. When the rate of divergence (Λ_1) exceeds the rates of convergence (Λ_2, Λ_3) an increase in fractal dimension and a change from smooth to nonsmooth fractal attrac-

tors takes place. The cross sections of these nonsmooth attractors may be striated, checkered, or spiral-like structures, depending on the value of the stable complex eigenvalues.

Examples of different fractal types of chaotic attractors of a map similar to Eq. (1) were studied by Lorenz [8]. The application of the thermodynamical formalism for phase transitions to hyperbolic dynamical systems with different fractal types of attractors have been discussed by Paoli, Politi, and Badii [9]. We can show that the present map exhibits dynamical behavior equivalent to a map version of the solenoid [10]. The cross sections of the attractors are also equivalent to attractors obtained by the complex iterated function system (IFS) $z' = Az \pm 1$ [11]. Comparison with these results suggests that the Mandelbrot set obtained for the geometric transition from disconnected to connected in the IFS also occurs in our context of explicit dynamical systems. We predict that attractors of the type shown in Figs. 4(h) and 4(i) with the cross-section property disconnected and connected, respectively, can be realized in deterministic dynamical systems with three invertible map dimensions or four continuous variables. We note, however, that the examples of the piecewise-linear mapping equation (1) are ideal in the sense that they possess uniform directions of convergence and divergence. Nevertheless, our results can be transduced to the more general class of nonlinear maps. In nonlinear systems, the cross sections additionally depend on local scaling and are therefore simply distorted versions of the totally self-similar examples found in the piecewise-linear map. We suggest that the idea of *dynamical* properties determining *geometric* fractal properties is universal in the sense that all dynamical systems that fulfill the fundamental properties of stretching and folding acting on a contracting dynamics exhibit the outlined qualitative behavior.

*Present address: Staedelschule, Institute for New Media, D-60314 Frankfurt, Germany.

[1] O. E. Rössler, Z. Naturforsch. Teil A **38**, 788 (1983).

[2] M. Klein and G. Baier, in *A Chaotic Hierarchy*, edited by G. Baier and M. Klein (World Scientific, Singapore, 1991).

[3] G. Baier and M. Klein, Phys. Lett. A **177**, 32 (1993).

[4] M. Klein and G. Baier, Physica A **191**, 564 (1992).

[5] A. Kittel, J. Peinke, M. Klein, G. Baier, J. Parisi, and O. E. Rössler, Z. Naturforsch. Teil A **45**, 1377 (1990).

[6] J. Peinke, M. Klein, A. Kittel, G. Baier, J. Parisi, R. Stoop, J. L. Hudson, and O. E. Rössler, Europhys. Lett. **14**, 615 (1991).

[7] J. Kaplan and J. A. Yorke, in *Functional Differential Equations and Fixed Points*, edited by H.-O. Peitgen and H.-O. Walther, Lecture Notes in Mathematics Vol. 730 (Springer, Berlin, 1979).

[8] E. N. Lorenz, Physica **17D**, 279 (1985).

[9] P. Paoli, A. Politi, and R. Badii, Physica D **36**, 263 (1989).

[10] S. Smale, in *Turbulence Seminar*, edited by P. Bernard and T. Ratiu, Lecture Notes in Mathematics Vol. 615 (Springer, Berlin, 1977).

[11] M. Barnsley, *Fractals Everywhere* (Academic, San Diego, CA, 1988).